Journal of Alloys and Compounds 487 (2009) 758–762

Contents lists available at ScienceDirect

Journal of Alloys and Compounds

journal homepage: www.elsevier.com/locate/jallcom

# Synthesis process and luminescence properties of $Tm^{3+}$ in $AWO_4$ (A = Ca, Sr, Ba) blue phosphors

Jinsheng Liao*, Bao Qiu, Herui Wen, Jinglin Chen, Weixiong You, Liangbin Liu

*School of Material and Chemistry Engineering, Jiangxi University of Science and Technology, Ganzhou, Jiangxi 341000, China*

ARTICLE INFO

*Article history:*
Received 4 May 2009
Received in revised form 14 August 2009
Accepted 14 August 2009
Available online 22 August 2009

*Keywords:*
Optical material
Chemical synthesis
Luminescence

ABSTRACT

$AWO_4:Tm^{3+}$ (A = Ca, Sr and Ba) blue phosphors were prepared via a mild and facile hydrothermal route. X-ray diffraction (XRD), scanning electron microscope (SEM), photoluminescence excitation and emission spectra and decay curve were used to characterize the $AWO_4:Tm^{3+}$ phosphors. By analyzing the excitation and emission spectra of $AWO_4$:Tm and undoped $AWO_4$ samples, the result indicates that there exists the energy transfer from the $WO_4^{2-}$ group to the $Tm^{3+}$ ion only in $CaWO_4$:Tm phosphor. The luminescence decay curves from the $^1D_2$ state of $Tm^{3+}$ in $AWO_4$ phosphors show bi-exponential characteristics when excited directly to the $^1D_2$ state, implying that there exist two luminescence centers in $AWO_4$:Tm phosphors. Because $AWO_4:Tm^{3+}$ phosphors exhibit intensive blue emission and high color purity under UV excitation, it is considered to be a new promising blue phosphor for field emission display application.

## 1. Introduction

Recently, rare-earth activated inorganic material has been widely employed in some important applications, such as fluorescent lamps [1–4], solid-state lasers [5–8], scintillators [9,10], and field emission display (FED) [11–14]. It is very important to develop novel phosphors for the important field of FED application [11]. However, there are not many examples of new phosphors which have been designed for FED. It has been difficult to find a suitable blue phosphor [12]. At present, the most efficient blue phosphors contain sulfur in the host material composition [15,16], for example, ZnS, $ZnSO_4$ and $Y_2O_2S$. Although they have good luminescence performances, the lifetime of the display is limited by the degradation of these sulfide phosphors during FED operation [11,12]. With a motivation to develop a new blue phosphor, tungstate-based phosphor may emerge as an alternate choice for blue phosphor, due to their superior chemical and thermal stability [17].

The alkaline-earth metal tungstates $AWO_4$ ($A = Ca^{2+}, Sr^{2+}, Ba^{2+}$) have been extensively investigated as a self-activating phosphor emitting blue or green light under ultraviolet or X-ray excitation [18,19]. The full-width at half-maximum of blue emission is broad in $AWO_4$ phosphor (about 100 nm) [18], which is disadvantage to improve the color purity. At present, $AWO_4$ were reported to be efficient luminescent hosts for rare earth [20–23]. $Tm^{3+}$ ion is widely used as activator of blue emission corresponding to its $^1D_2 \rightarrow {}^3F_4$ and $^1G_4 \rightarrow {}^3H_6$ transitions [24–29]. Their luminescence spectra consist of several very narrow bands, which make them effective luminescent centers. These investigations of $Tm^{3+}$-doped materials mainly focused on host matrix, such as fluorides [25], phosphates [27], and vanandates [28]. However, to the best of our knowledge, there is no study that has been devoted to the luminescence properties of $AWO_4$:Tm phosphors.

In this paper, $AWO_4$:Tm blue phosphors were synthesized by the mild hydrothermal method. The energy transfer from the $WO_4^{2-}$ group to the $Tm^{3+}$ ions is investigated in the $AWO_4$:Tm phosphors based on the luminescence properties of $AWO_4$:Tm and undoped $AWO_4$ samples. The $^1D_2$ excited-state dynamics of $Tm^{3+}$ in $AWO_4$ phosphors were analyzed by utilizing the double-exponential function. The blue emission in the visible range were observed in $AWO_4$:Tm phosphors. The high color purity of the luminescence in $AWO_4$:Tm phosphors was suggested as a blue phosphor for FED application.

## 2. Experimental

### 2.1. Preparation

Analytical reagent (AR) chemicals of $A(NO_3)_2$ (A = Ca, Sr, and Ba), $Na_2WO_4 \cdot 2H_2O$, citric acid, $HNO_3$ and NaOH were purchased from Shanghai Chemical Industrial Co., and used as the starting materials without any further purification. A procedure for the sample synthesis is typically described as follows: 0.25 mmol $Tm(NO_3)_3 \cdot 6H_2O$ with purity of 99.99% was first dissolved in deionized water under heating to obtain solution. Meanwhile 4.5 mmol $A(NO_3)_2$ and 2.5 mmol citric acid as chelating agent for the metal ions were added into the $Tm(NO_3)_3$ solution while stirring. Second, 5 mmol $Na_2WO_4 \cdot 2H_2O$ was slowly added to the mixed solution until little white precipitate formed (when the pH value of solution is about 3, white precipitate

---

* Corresponding author. Fax: +86 797 8312204.
*E-mail address:* jsliao1209@126.com (J. Liao).

0925-8388/$ – see front matter © 2009 Elsevier B.V. All rights reserved.
doi:10.1016/j.jallcom.2009.08.068

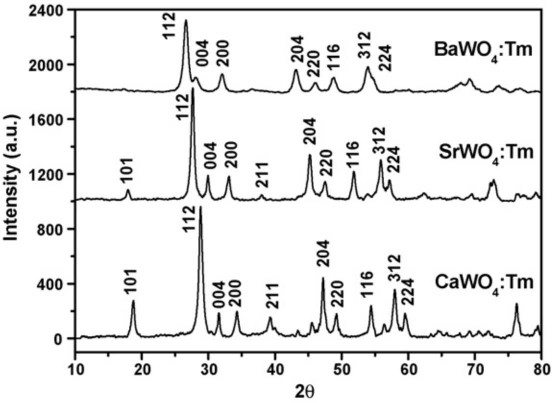

**Fig. 1.** XRD spectra for AWO$_4$:Tm (A = Ca, Sr and Ba) sample prepared by hydrothermal method.

is polytungstate species). A well-controlled amount of NaOH solution was then added with magnetic stirring to pH 9 to form a little white precipitate (white precipitate is monotungstate species) [30,31]. The precipitate was transferred into a Teflon-lined stainless-steel autoclave, and heated to 180 °C for 12 h. Then the autoclave was cooled to room temperature naturally. The white powders obtained were washed three times by dispersing in deionized water and ethanol and followed by the centrifugation. The white powder products were dried in air at 100 °C for 4 h. To investigate the energy transfer from the WO$_4^{2-}$ group to the Tm$^{3+}$ ions in AWO$_4$:Tm phosphors, undoped AWO$_4$ samples were prepared by the same procedure.

### 2.2. Characterization

The crystal structural characterization and phase identification of the as-prepared samples were carried out using a PANalytical X'Pert Pro X-ray diffractometer (XRD) with Cu K$\alpha_1$ radiation ($\lambda$ = 0.154187 nm) for 2$\theta$ ranging from 10° to 80°. The particle size and morphology of the samples were inspected using scanning electronic microscope (SEM Philips XL30). The photoluminescence spectra in the visible region and the luminescence decay were recorded on an Edinburgh Instruments FLS920 spectrofluorimeter equipped with both continuous (450 W) xenon and pulsed xenon (nanosecond) lamps. All spectra were corrected for the intensities as well as the line positions. All measurements were performed at room temperature.

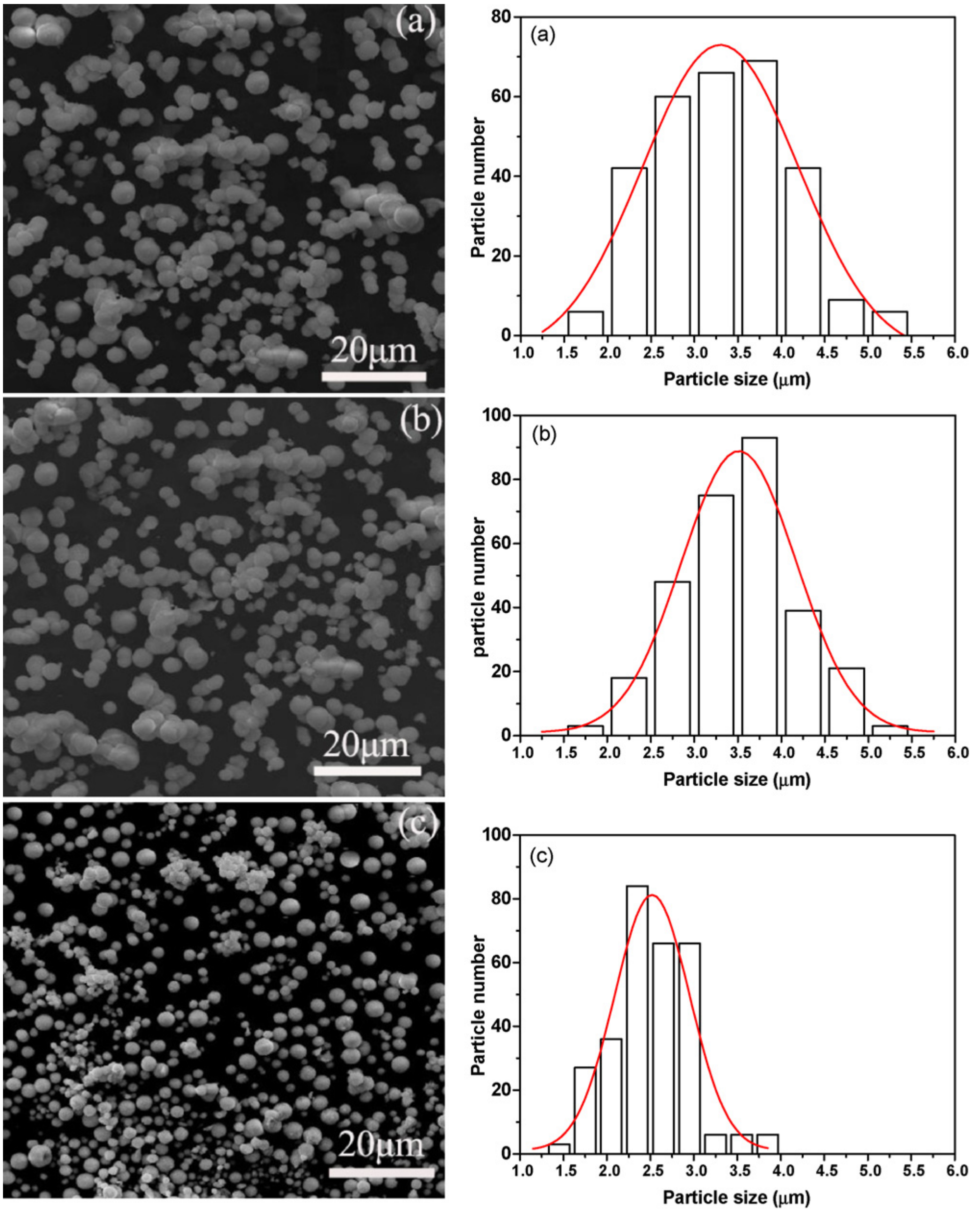

**Fig. 2.** SEM image (left) and particle size distributions (right) of the AWO$_4$:Tm (A = Ca, Sr and Ba) sample. (a) CaWO$_4$:Tm, (b) SrWO$_4$:Tm and (c) BaWO$_4$:Tm.

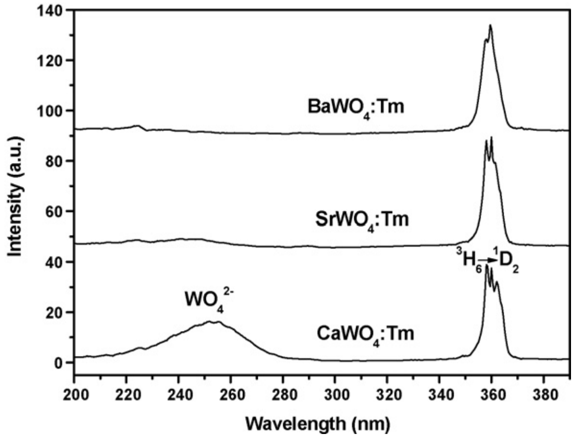

**Fig. 3.** Excitation spectra of AWO$_4$:Tm (A = Ca, Sr and Ba) sample, monitoring the Tm$^{3+}$ emission at 453 nm.

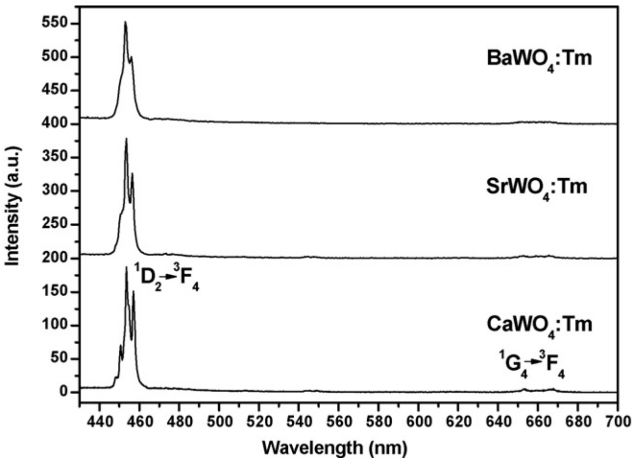

**Fig. 5.** Emission spectra of AWO$_4$:Tm (A = Ca, Sr and Ba) samples under direct excitation of 358 nm at room temperature.

## 3. Results and discussion

The crystallinity and phase purity of the as-prepared samples are examined with XRD. Fig. 1 presents XRD patterns of the AWO$_4$:Tm (A = Ca, Sr and Ba) samples. From Fig. 1, it can be seen that all diffraction peaks matched well the standard data of scheelite phase AWO$_4$ (A = Ca, Sr and Ba) (Joint Committee for Power Diffractions Standards, JCPDS card NO. 41-1431, 85-0587 and 43-0646). Their strongest intensity peaks diffracted from the same plane assigned as (1 1 2). They have scheelite structure with tetragonal crystal system and $I4_1/a$ space group. No additional diffractions that could be attributed to impurities are observed. Therefore, all as-prepared samples are pure phase. The peaks of the XRD patterns for BaWO$_4$:Tm phosphor become broader than those of CaWO$_4$:Tm and SrWO$_4$:Tm phosphors (Fig. 1), it is indicated that the crystal size of BaWO$_4$:Tm phosphor is the smallest among AWO$_4$:Tm phoshors. SEM image (the left of Fig. 2) shows that the three samples composed of a number of monodispersed microparticles with spherical shape. The particle size distribution (the right of Fig. 2) was counted from SEM images. The distributions are very close to the normal curves. They are in ranges of 1.75–5.22, 1.95–5.36, and 1.48–3.97 µm with the average of 3.30 ± 1.73, 3.48 ± 1.70, and 2.52 ± 1.24 µm in diameter for CaWO$_4$:Tm, SrWO$_4$:Tm and BaWO$_4$:Tm phosphors, respectively. The average size of BaWO$_4$:Tm phosphors is smaller than that of CaWO$_4$:Tm and SrWO$_4$:Tm phosphors. The results of SEM agree with those of XRD.

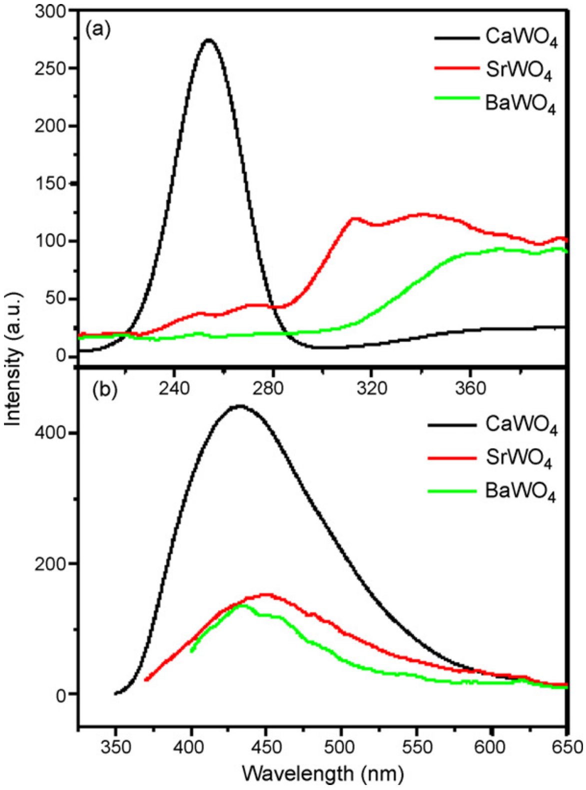

**Fig. 4.** Excitation (a) and emission (b) spectra of AWO$_4$ (A = Ca, Sr and Ba) sample (for excitation spectra, monitoring the WO$_4{}^{2-}$ group 440 nm; for emission spectra, the excitation wavelengths are 255, 310, and 358 nm corresponding to CaWO$_4$, SrWO$_4$, and BaWO$_4$, respectively).

Fig. 3 shows the excitation spectra of AWO$_4$:Tm phosphors by monitoring the room temperature emission at 453 nm due to the $^1D_2 \rightarrow {}^3F_4$ transition. It can be clearly seen that the excitation spectra of CaWO$_4$:Tm phsophor consist of a broad band from 210 to 290 nm with a maximum at about 255 nm, which electrons are excited from the oxygen 2p states to tungsten 5d states through the absorption of photons within the WO$_4{}^{2-}$ group [32]. In the excitation spectra of SrWO$_4$:Tm and BaWO$_4$:Tm phosphors, the relative intensities of charge-transfer band (W$^{6+}$–O$^{2-}$) are much weaker than that of CaWO$_4$:Tm phosphor. The results indicate that CaWO$_4$:Tm phosphor is the most effective for the energy transfer from the WO$_4{}^{2-}$ group to the Tm$^{3+}$ ions in AWO$_4$:Tm phosphors (discussed in next paragraph). In the longer wavelength region, the f–f transitions within the Tm$^{3+}$ 4f$^{12}$ configuration can be detected with stronger intensity with respect to charge-transfer transition, which is assigned as transition from the $^3H_6$ ground state to the $^1D_2$ excited state of Tm$^{3+}$ located from 340 to 370 nm with several sharp lines.

To investigate energy transfer from the WO$_4{}^{2-}$ group to the Tm$^{3+}$ ions in AWO$_4$:Tm phosphors, the excitation and emission spectra for undoped AWO$_4$ samples are shown in Fig. 4. It can be clearly seen that CaWO$_4$ samples have strong and broad excitation peak at about 255 nm (39,215 cm$^{-1}$). Since the energy gap between the WO$_4{}^{2-}$ group and the excited state $^3P_2$ (~38,315 cm$^{-1}$) of Tm$^{3+}$ [33] is about 900 cm$^{-1}$ and the maximum phonon energy of AWO$_4$ crystal is about 900 cm$^{-1}$ [18], the probability of the energy transfer from the WO$_4{}^{2-}$ group to the excited state $^3P_2$ of Tm$^{3+}$ is great via one phonon-assisted process in the CaWO$_4$:Tm phosphors. For SrWO$_4$ sample, the energy gap between its weak excitation peak at 310 nm (32,258 cm$^{-1}$) and the excited state $^1D_2$ (27,933 cm$^{-1}$) of Tm$^{3+}$ [33] is 4325 cm$^{-1}$, the energy transfer from the WO$_4{}^{2-}$ group to the excited state $^1D_2$ of Tm$^{3+}$ is nearly impossible occurred

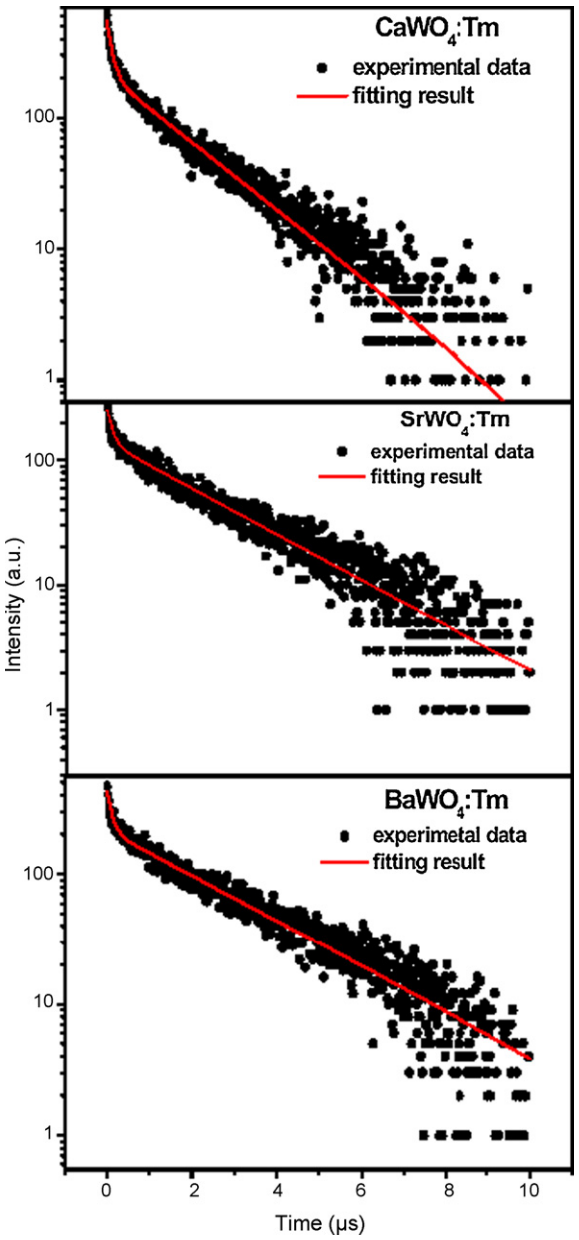

**Fig. 6.** Luminescence decay of $^5D_0$ state of AWO$_4$:Tm (A = Ca, Sr and Ba) sample (excitation wavelength 358 nm, monitoring the Tm$^{3+}$ emission at 453 nm).

via five phonon-assisted process in the SrWO$_4$:Tm phosphors. For BaWO$_4$ sample, although the energy of its excitation peak at 358 nm matches with the excited state $^1D_2$ of Tm$^{3+}$, the absorption peak of BaWO$_4$ sample is too weak to transfer the energy from the WO$_4{}^{2-}$ group to the excited state $^1D_2$ of Tm$^{3+}$. Therefore, the energy transfer from the WO$_4{}^{2-}$ group to the Tm$^{3+}$ ions is observed only in the CaWO$_4$:Tm phosphors.

Fig. 5 shows the emission spectra of 5 at.% AWO$_4$:Tm phosphors under the excitation of continuous Xe-lamp irradiation (358 nm) at room temperature. The strong blue emission band centered at 453 nm is observed from all samples. It corresponds to the emission from $^1D_2$ state to the $^3F_4$ state. The other very weak band is also present at 650 nm assigned to $^1G_4 \rightarrow {}^3F_4$ transition, while the transition of $^1G_4 \rightarrow {}^3H_6$ at about 470 nm is too weak to detect in AWO$_4$:Tm phosphors. Therefore, the strongest emission of Tm$^{3+}$ in AWO$_4$ phosphors is $^1D_2 \rightarrow {}^3F_4$ transition in blue region, showing that high color purity of the luminescence whose CIE chromaticity color coordinates were (0.158, 0.064), (0.159, 0.063), and (0.157, 0.065) corresponding to CaWO$_4$:Tm, SrWO$_4$:Tm, and BaWO$_4$:Tm, respectively.

**Table 1**
The double-exponential fitting parameters of AWO$_4$:Tm phosphors.

| AWO$_4$:Tm | $A_1$ | $\tau_1$ (μs) | $A_2$ | $\tau_2$ (μs) | $\tau_{av}$ (μs) |
|---|---|---|---|---|---|
| CaWO$_4$:Tm | 342 | 0.122 | 215 | 1.69 | 1.53 |
| SrWO$_4$:Tm | 120 | 0.118 | 139 | 2.34 | 2.25 |
| BaWO$_4$:Tm | 214 | 0.111 | 216 | 2.52 | 2.42 |

The luminescence lifetime of the $^1D_2$ state was measured under the excitation at 358 nm, and the decay curve deviated significantly from single exponential. It is suggested that the non-exponential dynamics are contributed by two different luminescent Tm$^{3+}$ centers. The process has also been observed in Yb$^{3+}$, Er$^{3+}$-codoped PbWO$_4$ powder [34], which is the same scheelite structure as AWO$_4$. The decay curve for $^1D_2 \rightarrow {}^3F_4$ (453 nm) of Tm$^{3+}$ ions can be well fitted into a double-exponential function as $I = A_1 \exp(-t/\tau_1) + A_2 \exp(-t/\tau_2)$ ($\tau_1$ and $\tau_2$ are fast and slow components of the luminescence lifetimes, respectively. $A_1$ and $A_2$ are the fitting parameters), and fitting curves are shown in Fig. 6 in semilog scale. The fitting parameters are listed in Table 1. It can be seen from Table 1 that the short lifetimes ($\tau_1$) of AWO$_4$:Tm are nearly same (about 0.12 μs), while the long lifetimes ($\tau_2$) are different. The short lifetimes are expected for the surface site because the surface defects or impurity ligands such as OH$^-$ in samples might act as the channels of nonradiative relaxation. The difference of the long lifetimes is expected for the lattice site because Tm$^{3+}$ ions locate different lattice environment. The average lifetimes for $^1D_2$ energy level of Tm$^{3+}$ ions are about 1.53, 2.25, and 2.42 μs for CaWO$_4$:Tm, SrWO$_4$:Tm, and BaWO$_4$:Tm, respectively, as determined by the formula as $\tau_{av} = (A_1\tau_1^2 + A_2\tau_2^2)/(A_1\tau_1 + A_2\tau_2)$ [35].

For further identifying the two Tm$^{3+}$ luminescence centers in AWO$_4$:Tm, the site-selective spectroscopy at low temperature, may also be taken into consideration, for which additional measurements would be required. These will be the subjects of our future study.

## 4. Conclusions

In summary, we have prepared Tm$^{3+}$-activated AWO$_4$ (A = Ca, Sr and Ba) blue phosphors by the mild hydrothermal method. The SEM photograph demonstrated that the crystalline particles are nearly monodisperse and spherical shape. By analyzing excitation and emission spectra of AWO$_4$:Tm and undoped AWO$_4$ samples, the result indicates that there exists the energy transfer from the WO$_4{}^{2-}$ group to the Tm$^{3+}$ ion only in CaWO$_4$:Tm phosphor. The blue emissions for the Tm$^{3+}$ ions decay bi-exponentially, suggesting that there exists two luminescence centers in the AWO$_4$:Tm phosphor, i.e. the surface and lattice sites. The characteristic of Tm$^{3+}$ ions of f–f transitions is observed upon UV excitation. Among these transitions, it is found that the $^1D_2 \rightarrow {}^3F_4$ transition with blue emission is strong, while the other transitions are too weak to affect the intensity and chromaticity of blue emission. Therefore, the high color purity of luminescence and easy preparation of these systems make them potential candidates for FED application.

## Acknowledgements

This work has been financially supported by Ganzhou City Public Services Platform for Technical Innovation of Nonferrous Metal and the National Natural Science Foundation of China.

## References

[1] J.G. Li, X.D. Li, X.D. Sun, T. Ishigaki, J. Phys. Chem. C 112 (2008) 11707.
[2] F. Lei, B. Yan, J. Solid State Chem. 181 (2008) 855.
[3] Z. Chen, Y.W. Yan, J.M. Lin, Y. Yin, H.M. Wen, G.H. Liao, C.L. Wu, J.Q. Zao, D.H. Liu, H.M. Tian, C.S. Zhang, S.D. Li, J. Alloys Compd. 478 (2009) 679.
[4] J.S. Liao, B. Qiu, H. Wen, W. You, Opt. Mater. 31 (2009) 1513.
[5] H. Zhou, X.H. Ma, G.T. Chen, W.C. Lv, Y. Wang, Z.Y. You, J.F. Li, Z.J. Zhu, C.Y. Tu, J. Alloys Compd. 475 (2009) 555.
[6] J.H. Huang, Y.J. Chen, Y.F. Lin, X.H. Gong, Z.D. Luo, Y.D. Huang, Opt. Lett. 33 (2008) 2548.
[7] Y. Yang, Y.L. Lu, J. Wang, Y.B. Dai, B.D. Sun, J. Alloys Compd. 453 (2008) 482.
[8] X.Y. Huang, G.F. Wang, J. Alloys Compd. 475 (2009) 693.
[9] A. Nosenko, L. Kostyk, L. Koslovska, J. Lumin. 90 (2000) 49.
[10] S.A. Cicillini, A.M. Pires, O.A. Serra, J. Alloys Compd. 374 (2004) 169.
[11] J.H. Hao, M. Cocivera, Appl. Phys. Lett. 79 (2001) 740.
[12] H. Wang, C.K. Lin, X.M. Liu, J. Lin, Appl. Phys. Lett. 87 (2005) 181907.
[13] N. Hirosaki, R.J. Xie, K. Kimoto, Appl. Phys. Lett. 86 (2005) 211905.
[14] P. Psuja, D. Hreniak, W. Strek, J. Alloys Compd. 451 (2008) 571.
[15] P.H. Holloway, J. Sebastian, T. Trottier, H. Swart, R.O. Petersen, Solid State Technol. 38 (1995) 47.
[16] T. Hisamune, Processing of the Ninth International Displays Workshops, 2002, p. 685.
[17] H.L. Li, Z.L. Wang, J.H. Hao, Mater. Sci. Eng. 1 (2009) 012010.
[18] T. Thongtem, A. Phuruangrat, S. Thongtem, Appl. Surf. Sci. 254 (2008) 7581.
[19] L.S. Cavalcante, J.C. Sczancoski, J.W.M. Espinosa, J.A. Varela, P.S. Pizani, E. Longo, J. Alloys Compd. 474 (2009) 195.
[20] J.S. Liao, B. Qiu, H.R. Wen, J.L. Chen, W.X. You, Mater. Res. Bull. 44 (2009) 1863.
[21] Y.G. Su, L.P. Li, G.S. Li, Chem. Mater. 20 (2008) 6060.
[22] X.M. Lou, D.H. Chen, Mater. Lett. 62 (2008) 1681.
[23] V.B. Mikhailik, H. Kraus, G. Miller, M.S. Mykhaylyk, D. Wahl, J. Appl. Phys. 97 (2005) 083523.
[24] A.N. Kuzmin, A.V. Kachynski, P.N. Prasad, A.A. Demidovich, L.E. Balay, A. Bednarkiewicz, W. Strek, A.N. Titov, J. Appl. Phys. 95 (2004) 7862.
[25] F. Vetrone, V. Mahalingam, J.A. Capobianco, Chem. Mater. 21 (2009) 1847.
[26] C.P. Ortiz, D.M. Boye, J. Lumin. 128 (2008) 894.
[27] R. Pang, C.Y. Li, L.H. Jiang, Q. Su, J. Alloys Compd. 471 (2009) 364.
[28] H.W. Zhang, X.Y. Fu, S.Y. Niu, G.Q. Sun, Q. Xin, Solid State Commun. 132 (2004) 527.
[29] E.B. Mejia, J. Appl. Phys. 100 (2006) 113110.
[30] C.F. Baes, J.R.E. Mesmer, The Hydrolysis of Cations, Wiley, New York, 1976.
[31] S.J. Chen, J.H. Zhou, X.T. Chen, J. Li, L.H. Li, J.M. Hong, Z.L. Xue, X.Z. You, Chem. Phys. Lett. 375 (2003) 185.
[32] C.A. Kodaira, H.F. Brito, M.C.F.C. Felinto, J. Solid State Chem. 171 (2003) 401.
[33] X.H. Ma, Z.Y. You, Z.J. Zhu, J.F. Li, B.C. Wu, Y. Wang, C.Y. Tu, J. Alloys Compd. 465 (2008) 406.
[34] Q. Dai, H. Song, X. Ren, S. Lu, G. Pan, X. Bai, B. Dong, R. Qin, X. Qu, H. Zhang, J. Phys. Chem. C 112 (2008) 19694.
[35] S. Mukarami, H. Markus, R. Doris, M. Makato, Inorg. Chim. Acta 300 (2000) 1014.